



# Structure, rheology and shear alignment of Pluronic block copolymer mixtures

Gemma E. Newby<sup>a,d</sup>, Ian W. Hamley<sup>a,\*</sup>, Stephen M. King<sup>b</sup>, Christopher M. Martin<sup>c</sup>, Nicholas J. Terrill<sup>d</sup>

<sup>a</sup> Department of Chemistry, University of Reading, Reading, RG6 6AD, UK

<sup>b</sup> ISIS, Science and Technology Facilities Council Rutherford Appleton Laboratory, Harwell Science and Innovation Campus, Didcot, OX11 0QX, UK

<sup>c</sup> Synchrotron Radiation Source, CLRC Daresbury Laboratory, Warrington, WA4 4AD, UK

<sup>d</sup> Diamond Light Source Ltd., Diamond House, Harwell Science and Innovation Campus, Chilton, Didcot, Oxfordshire, OX11 0DE, UK

## ARTICLE INFO

### Article history:

Received 3 July 2008

Accepted 19 September 2008

Available online 26 September 2008

### Keywords:

Pluronic

Rheology

Small-angle scattering

Shear alignment

## ABSTRACT

The structure and flow behaviour of binary mixtures of Pluronic block copolymers P85 and P123 is investigated by small-angle scattering, rheometry and mobility tests. Micelle dimensions are probed by dynamic light scattering. The micelle hydrodynamic radius for the 50/50 mixture is larger than that for either P85 or P123 alone, due to the formation of mixed micelles with a higher association number. The phase diagram for 50/50 mixtures contains regions of cubic and hexagonal phases similar to those for the parent homopolymers, however the region of stability of the cubic phase is enhanced at low temperature and concentrations above 40 wt%. This is ascribed to favourable packing of the mixed micelles containing core blocks with two different chain lengths, but similar corona chain lengths. The shear flow alignment of face-centred cubic and hexagonal phases is probed by *in situ* small-angle X-ray or neutron scattering with simultaneous rheology. The hexagonal phase can be aligned using steady shear in a Couette geometry, however the high modulus cubic phase cannot be aligned well in this way. This requires the application of oscillatory shear or compression.

© 2008 Elsevier Inc. All rights reserved.

## 1. Introduction

The most widely studied and commercially important amphiphilic block copolymers are the PEO-*b*-PPO-*b*-PEO triblocks, where PEO denotes poly(ethylene oxide) and PPO denotes poly(propylene oxide). These copolymers are manufactured by a number of companies [1,2], but best known by their BASF trade name Pluronics or as poloxamers. The properties of these materials have been extensively reviewed [3–7]. They are useful as biocompatible materials for biomedical and personal care applications where their gelation properties are exploited. The ability to tune the gel transition, for instance to enable slow release gel delivery systems, has been the focus of considerable attention. Use of mixtures of Pluronic block copolymers is one strategy to modulate structural and rheological properties, and this is the focus of the present paper.

At low temperature (<ca. 15 °C) both PEO and PPO are water soluble. As temperature is increased PPO becomes increasingly hydrophobic and micelles form. As temperature is increased further the PEO becomes less soluble, leading to shrinkage of the corona and above a critical solution temperature to phase separation and clouding. Micellization at fixed concentration occurs

above a critical micelle temperature (cmt) or at fixed temperature above a critical micelle concentration (cmc). At sufficiently high concentration, Pluronic copolymers are known to form lyotropic liquid crystal phases. These have various structures but are characterised by gel-type behaviour, i.e. the development of a measurable yield stress or elastic modulus. The term gel refers to a physically cross-linked network that results from the links between micelles that result from telechelic PEO chains tethered in two different micelles. Gelation is observed above a so-called critical gelation concentration (cgc).

Although the micellization and gelation of individual Pluronic copolymers has been extensively investigated, there have been far fewer studies on mixtures of Pluronics. Prior reports indicate that co-micellization is usually observed. For example, Jain et al. studied mixtures of E<sub>30</sub>P<sub>56</sub>E<sub>30</sub> (where E denotes ethylene oxide, P denotes propylene oxide and the subscripts are the degrees of polymerization) with six other Pluronics and observed co-micellization [8]. Co-micellization of F77 and F87 has also been reported, although either copolymer micellizes separately in mixtures with F127 [9]. Chaibundit et al. have investigated the micellization and gelation of mixtures of Pluronic P123 (E<sub>20</sub>P<sub>72</sub>E<sub>20</sub>) and F127 (E<sub>98</sub>P<sub>67</sub>E<sub>98</sub>) and observed the formation of mixed micelles with a narrow size distribution, for this case in which the copolymers have similar hydrophobic block lengths [10]. They also extensively review prior literature on the micellization of mixtures of PEO-based block copolymers.

\* Corresponding author at: Department of Chemistry, University of Reading, Reading, RG6 6AD, UK.

E-mail address: i.w.hamley@reading.ac.uk (I.W. Hamley).

Chu and co-workers have investigated the micellization of Pluronic F127 ( $E_{99}P_{69}E_{99}$ ) with the related triblock  $E_{45}B_{14}E_{45}$  in which the central butylene oxide (B) block is more hydrophobic [11]. At low temperature, the latter copolymer has a much lower cmc and addition of Pluronic F127 leads to incorporation of the chains into mixed micelles. The temperature dependence of the cmc of Pluronic F127 is greater than that of  $E_{45}B_{13}E_{45}$  and at high temperature Pluronic F127 has a lower cmc. Added  $E_{45}B_{13}E_{45}$  is therefore incorporated into the pre-existing F127 micelles. However, due to polydispersity there is a bimodal distribution of average micelle sizes. At an intermediate temperature where both copolymers have the same cmc, a single distribution of mixed micelles containing equal proportions of each copolymer is formed. A change in cubic micellar gel structure was also observed upon varying the composition of mixed micelles in this system [12]. Mixed micelles have also been observed in aqueous solution of diblock  $E_{60}B_{12}$  and triblock  $E_{55}B_{20}E_{55}$  [13]. Since the PEO block length is essentially the same, the dimensions of the mixed micelles were unaffected by mixture composition. The association number was found to be proportional to composition, when allowance was made for coronal chain looping of the triblock. The size distribution of mixed micelles was found to be narrower than that of the individual copolymer micelles, leading to a harder interaction potential. The association behaviour of mixtures of  $E_mB_nE_m$  and  $E_mS_nE_m$  (S denotes styrene oxide) block copolymers in aqueous solution has been probed by light scattering in dilute solution and rheometry in more concentrated solution [14]. The aim was to examine the effect of hydrophobicity of the mid-block (S has twice the hydrophobicity of B). Two distinct distributions of micelles were observed in 50:50 mixtures of copolymers with similar hydrophobic block lengths. However for micelles with dissimilar midblock lengths but similar hydrophobicity (i.e. S block approximately half the length of the B block) mixed micelles were observed with properties similar to those of the  $E_{82}S_9E_{82}$  micelles alone.

In the present paper, we report on the properties of gels formed by mixtures of Pluronic P85 and P123. In contrast to previous reports, this pair of Pluronics has quite different hydrophobic block lengths but similar PEO block lengths. The gel diagram of the binary system is mapped out using controlled stress shear rheometry. The structure of the gels is probed by small-angle X-ray scattering (SAXS) and small-angle neutron scattering (SANS) and shear alignment is probed, and for the case of the high temperature hexagonal-packed cylinder phase is correlated to changes in the viscoelasticity. We show that the gel properties, and phase behaviour, of the Pluronics can be modified by mixing these two copolymers, this may be useful in applications such as drug delivery or rheology modification.

## 2. Experimental

### 2.1. Materials

Pluronic copolymers P85 and P123 were used as received from BASF. The nominal compositions and molecular weights are P85:  $E_{26}P_{41}E_{26}$ ,  $M_w = 4600 \text{ g mol}^{-1}$ , P123:  $E_{20}P_{72}E_{20}$ ,  $M_w = 5750 \text{ g mol}^{-1}$  [7]. Uncertainties on degrees of polymerization are typically  $\pm 3$  [7]. Samples were fully dissolved in Millipore ultrafiltered water by stirring them in an ice bath and then they were left to equilibrate overnight at 4 °C. Mixture compositions of P85 and P123 (50/50 in this paper) are wt%/wt%. Mixtures were prepared by dissolving both polymers together in water.

### 2.2. Dynamic light scattering (DLS)

Measurements were carried out on well filtered solutions of copolymers (2 wt% in water) at 25 °C using an ALV/CGS-3 Com-

pact Goniometer System with ALV/LSE-5003 correlator using vertically polarized incident light of wavelength  $\lambda = 632.8 \text{ nm}$ . Measurements were performed at an angle  $\theta = 90^\circ$  to the incident beam and data were collected three times for 30 s. The intensity autocorrelation functions were analyzed by the constrained regularized CONTIN method [15] to obtain distributions of decay rates ( $\Gamma$ ), hence distributions of apparent mutual diffusion coefficient  $D_{app} = \Gamma/q^2$  [ $q = (4\pi n/\lambda) \sin(\theta/2)$ , where  $n$  is the refractive index of the solvent and  $\theta$  is the scattering angle], and ultimately of apparent hydrodynamic radius of the particle via the Stokes–Einstein equation

$$r_{h,app} = k_B T / (6\pi \eta D_{app}), \quad (1)$$

where  $k_B$  is the Boltzmann constant and  $\eta$  is the viscosity of water ( $\eta = 0.833 \text{ mPa s}$  at 28 °C and  $\eta = 0.720 \text{ mPa s}$  at 35 °C). The refractive index of water takes the value  $n = 1.332$  at 28 °C.

### 2.3. Rheology

Rheological properties were determined using a controlled stress AR-2000 rheometer (TA Instruments). A cone-and-plate geometry (cone diameter 60 mm, angle 2°) was used for all samples. Frequency scans were performed within the angular frequency range ( $\omega$ ) 0.5–600 rad/s, with the instrument in oscillatory mode at 25 °C. Preliminary strain sweeps were performed for each sample in order to define the linear viscoelastic region, thus ensuring that moduli were independent of strain.

### 2.4. Small-angle X-ray scattering (SAXS)

SAXS experiments on unaligned samples were performed on station 6.2 at the Synchrotron Radiation Source, Daresbury Lab, UK [16,17]. Samples contained in DSC pans modified to incorporate mica windows to allow transmission of the X-ray beam were mounted in a Linkam DSC cell of single pan design for thermal treatment. The X-ray wavelength was  $\lambda = 1.40 \text{ \AA}$  and the sample-detector distance was approximately 3.5 m. SAXS data were collected with a RAPID multiwire quadrant detector. Shear-alignment experiments were performed with a Physica MCR-501 rheometer in the cone-and-plate geometry on the Undulator beamline I22 at Diamond, Harwell Science and Innovation Campus, Didcot, UK. The X-ray wavelength was 1 Å, the sample-detector distance was approximately 3 m and data was collected with a RAPID multiwire 2D detector permitting the investigation of sample orientation. On both SAXS instruments, the wavenumber  $q = 4\pi \sin \theta / \lambda$  for SAXS was calibrated using rat-tail collagen.

### 2.5. Small-angle neutron scattering (SANS)

SANS experiments were performed on the LOQ diffractometer at the ISIS spallation neutron source, Rutherford Appleton Laboratory, Harwell Science and Innovation Campus, Didcot, UK. LOQ is a time-of-flight instrument which simultaneously uses a range of neutron wavelengths to cover a wide range of scattering vectors,  $q$ . In these experiments  $0.07 \leq q/\text{nm}^{-1} \leq 2.9$ , where  $q = 4\pi \sin(\theta)/\lambda$ ,  $2\theta$  is the scattering angle, and  $\lambda$  is the neutron wavelength. The SANS data were obtained for copolymer solutions in  $D_2O$  to reduce background scattering and maximise the contrast with the hydrogeneous copolymers. Data were corrected for the measured sample transmission and background scattering (using  $D_2O$  as a reference). The data were collected using a two-dimensional area detector permitting the investigation of sample orientation.

Shear alignment was investigated in two ways. Firstly, samples in a high temperature hexagonal-packed cylinder phase could be investigated with *in situ* rheometry using the Physica MCR-501

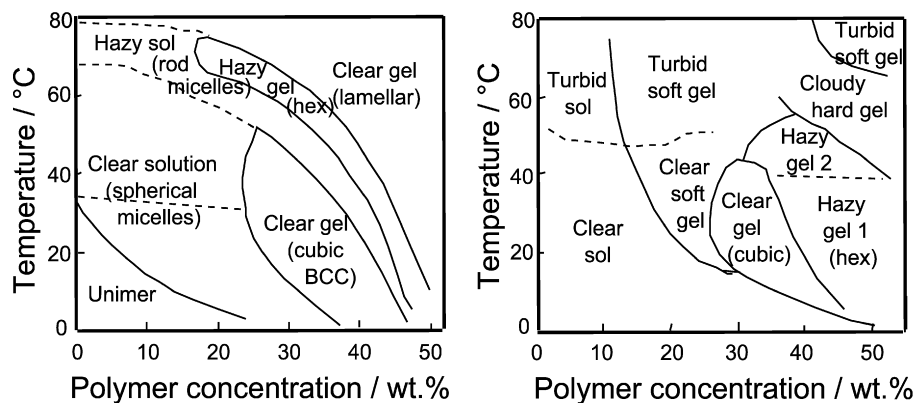


Fig. 1. Phase diagrams for P85 (left) and P123 (right).

**Table 1**  
Hydrodynamic radii from dynamic light scattering measurements.

Sample	Micellar $R_h$ (nm)	
	Measured	Literature
P85	$8.1 \pm 0.3$	$8.0^a$ , $8.0^b$
P123	$9.1 \pm 0.5$	$8.6^c$
P85/P123 50/50	$10.6 \pm 0.6$	–

<sup>a</sup> At 40 °C from Ref. [26].

<sup>b</sup> Thermodynamic radius from static light scattering at 35 °C from Ref. [27].

<sup>c</sup> At 30 °C and 40 °C from Ref. [10].

rheometer with a quartz Couette geometry (1 mm gap). Samples were subjected to continuous shear rates in the range 0.1 to  $5500 \text{ s}^{-1}$ . Temperature control was effected using a heated air stream. It proved impossible to shear high modulus cubic gels in the Physica rheometer. As an alternative, cubic gels were either “hand sheared” or subjected to steady shear in the MCR 501 rheometer using a cone-and-plate geometry. Both of these experiments were performed at room temperature. “Hand shearing” was done by manual oscillation of the sample placed between parallel quartz plates. These were subsequently wrapped in foil and mounted onto the sample holder in the neutron beam.

### 3. Results and discussion

#### 3.1. Micelle dimensions, rheology and gel diagram

Dynamic light scattering was used to determine micellar hydrodynamic radii. Table 1 summarises the results. The hydrodynamic radii values measured for micelles of P85 and P123 are in good agreement with values previously reported in the literature. For the 50/50 P85/P123 mixture, the hydrodynamic radius is larger than either of the parent polymers. This is agreement with the findings of Chaibundit et al. [10] for P123/F127 mixtures. The hydrodynamic radius passed through a maximum at an intermediate composition of the mixture, this resulting from interplay between an increase in association number with an increase in content of the shorter polymer and a decrease in length of coronal chains which stabilise the micelle size. In the case of P85/P123 mixed micelles, the corona chains are the same size and the increase in micelle size must result from the presence of PPO chains of different lengths in the micelle core. The shorter PPO chains in P85 may enable the longer PPO chains in P123 to adopt more extended conformations in a mixed micelle. The hydrodynamic radii are useful in our discussion of SAXS and SANS data from more concentrated solutions of the block copolymers (see following).

Phase diagrams for P85 and P123 have previously been reported and are summarised for convenience in Fig. 1. The phase diagram

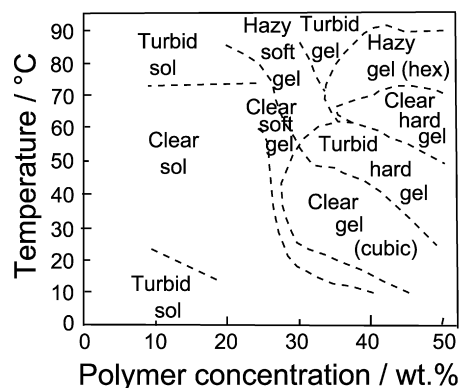
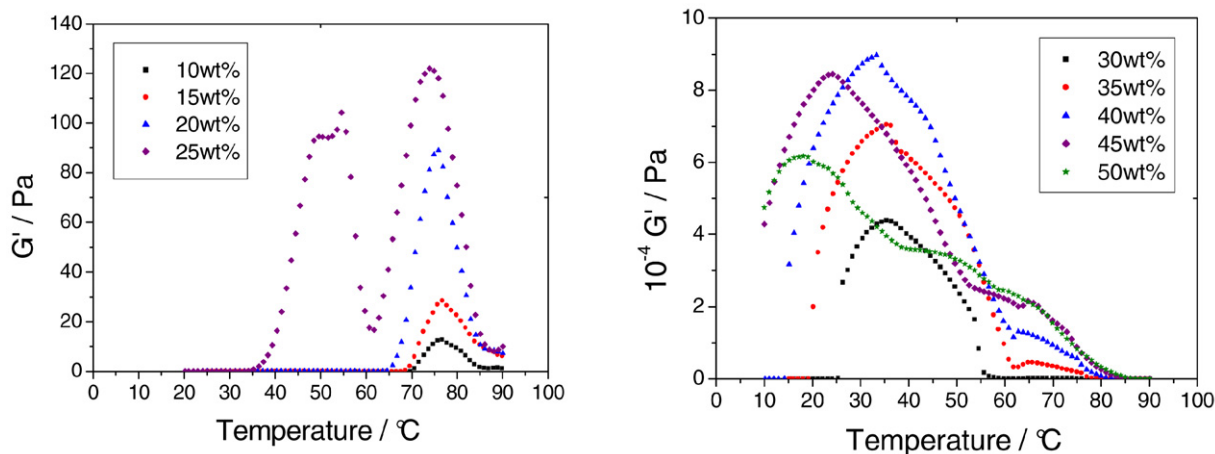


Fig. 2. Phase diagram for 50/50 mixtures of P85 and P123.

for P85 was obtained on the basis of our tube inversion and turbidity measurements, while structural assignments are taken from previous small-angle neutron scattering experiments [18,19]. The phase diagram for P123 is a gel diagram obtained from tube inversion flow tests and visual inspection [10], to which some structural assignments based on scattering experiments reported herein have been added. Since cubic phases in block copolymer solutions are clear hard gels, the cubic phase region in Fig. 1a can be labelled accordingly, and the micellar solution will be a clear sol. Regions of rod-like micellar solution or hexagonal phase are often turbid (see Fig. 1b). The dashed line in the P85 phase diagram at low concentrations separates regions of micellar solutions (above) and micellar/polymer coexistence (below). The dashed line between hazy gel 1 and 2 in the phase diagram for P123 separates regions where the gel is birefringent (below) from where it is not (above). The birefringence results from the presence of hexagonally-packed cylindrical micelles [10].

We have determined the phase diagram for a 50/50 mixture of P85 and P123, and this is presented in Fig. 2. The concentration indicated here and elsewhere is that of total copolymer in aqueous solution. The phase diagram comprises data from tube inversion flow tests with visual inspection, shear rheometry and small-angle scattering experiments. The solid lines are based on small-angle scattering and rheometry, while the dashed lines indicated boundaries between clear and turbid or hazy gels or solutions based on visual inspection. The topology of the phase diagram is similar to that for the parent polymers. A main difference is the absence of a hexagonal phase at low temperatures and high concentrations, this structure only being observed at higher temperature for 40 and 45 wt% copolymer solutions. The transition to a hexagonal phase is usually ascribed to an increase in association number which causes a spherical micelle core to expand until



**Fig. 3.** Temperature dependence of dynamic elastic shear modulus for 10 wt% to 50 wt% P85/P123 50/50 aqueous solutions. The experiments were carried out at a heating rate of 1 °C/min at an amplitude of 0.2% strain and an angular frequency of  $2\pi$  rad.

its radius exceeds that of a fully stretched chain [7]. The absence of a hexagonal phase in the P85/P123 system at high concentrations may be due to the release of packing constraints afforded by the presence of mixed micelles containing hydrophobic blocks of different lengths. For the F127/P123 system, addition of P123 with shorter coronal chains leads to destabilisation of the cubic gel phase, both in terms of increasing the critical gel concentration (lower concentration boundary of cubic phase) and by reducing the upper temperature boundary of the gel phase [10]. This is presumably due to the decreased size and hence effective volume fraction of the mixed micelles on increasing the P123 fraction. DLS measurements in dilute solution indicate that the hydrodynamic radius decreases above around 30 wt% P123. It is unclear from that work (which did not include structural studies in the gel phase) to what extent the micelle size and association number differ in dilute and concentrated (gel) phases. The gel boundary results suggest a continuous decrease in effective micelle size with increase in P123 content in the F127/P123 mixed system. In contrast, for mixtures of E<sub>45</sub>B<sub>14</sub>E<sub>45</sub> and E<sub>62</sub>P<sub>39</sub>E<sub>62</sub> (Pluronic F87), the minimum concentration for hard gel formation was higher than that for either individual copolymer, consistent with the observed separate micellization of the copolymers in dilute solution [20]. This is due to the large difference in cmcs for the two copolymers—E<sub>45</sub>B<sub>14</sub>E<sub>45</sub> micellizes at much lower concentrations, followed by the independent micellization of F87 at much higher concentration. In our case, mixed micelles are formed and the lower concentration stability limit of the cubic gel phase in the P85/P123 mixed system is similar to that of the parent homopolymers, for both of which the critical gel concentration is around 25 wt%. The stability region of the cubic gel phase is however enhanced compared to either homopolymer at higher concentration. This is ascribed to the release of packing constraints on core chains in the mixed micelles with the bimodal distribution of chain lengths, as discussed above.

The rheology data used, along with the other data, to delineate phase boundaries in Fig. 2 is presented in Fig. 3. The solutions with 20 wt% copolymer and below show an increase in modulus (to a few 10's of Pa) at high temperature, which is related to the formation of a soft gel of cylindrical micelles, as reported for many other Pluronic systems [7] and discussed further for our system shortly. The 25 wt% solution shows an additional soft gel phase at lower temperature, extending from around 40–65 °C. The data for solutions containing 30 wt% copolymer or more are shown in Fig. 3b. There is a dramatic increase in shear modulus for the low temperature gel phase, consistent with tube inversion flow tests which indicate formation of self-supporting gels in a certain tem-

**Table 2**

Observed SAXS reflections.

Concentration, temperature	Peak positions (Å <sup>-1</sup> )	Assignment	Structure
P85/P123 50/50			
30 wt%, 41 °C	0.0505 0.0727 0.0859	v. weak $q^*$ $\sqrt{4/3}q^*$	FCC
30 wt%, 70 °C	No Bragg peaks		
35 wt%, 36 °C	0.0472 0.0535 0.0768	$q^*$ $\sqrt{4/3}q^*$ $\sqrt{8/3}q^*$	FCC
35 wt%, 70 °C	0.0417 0.0729 0.0838	$q^*$ $\sqrt{3}q^*$ $\sqrt{4}q^*$	Hexagonal
40 wt%, 33 °C	0.0490 0.0549 0.0793	$q^*$ $\sqrt{4/3}q^*$ $\sqrt{8/3}q^*$	FCC
40 wt%, 70 °C	0.0433 0.0755 0.0868	$q^*$ $\sqrt{3}q^*$ $\sqrt{4}q^*$	Hexagonal
45 wt%, 25 °C	0.0486 0.0548 0.0842	$q^*$ $\sqrt{4/3}q^*$ $\sqrt{3}q^*$	FCC
45 wt%, 70 °C	0.0471 0.0819 0.0941	$q^*$ $\sqrt{3}q^*$ $\sqrt{4}q^*$	Hexagonal
P123			
20 wt%, 30 °C	No Bragg peaks		
20 wt%, 60 °C	No Bragg peaks		
35 wt%, 25 °C	0.0432 0.0495 0.0699	$q^*$ $\sqrt{4/3}q^*$ $\sqrt{8/3}q^*$	FCC
35 wt%, 45 °C	0.0401 0.0643 0.0997	$q^*$ $\sqrt{8/3}q^*$ $\sqrt{3}$	FCC?
35 wt%, 70 °C	No Bragg peaks		
40 wt%, 40 °C	0.0428 0.0749 0.0870	$q^*$ $\sqrt{3}q^*$ $\sqrt{4}q^*$	Hexagonal
P85			
40 wt%, 25 °C	0.0581 0.0617 0.0658 0.0848	$q^*$ ? $\sqrt{4/3}q^*$ $\sqrt{2}q^*$	FCC (predominant) + Hexagonal
40 wt%, 60 °C	0.0546 0.0946 0.1092	$q^*$ $\sqrt{3}q^*$ $\sqrt{4}q^*$	Hexagonal

perature range. The onset of the hard gel occurs at successively lower temperatures as the concentration is increased. The maximum gel stiffness increases with concentration up to 40–45 wt%

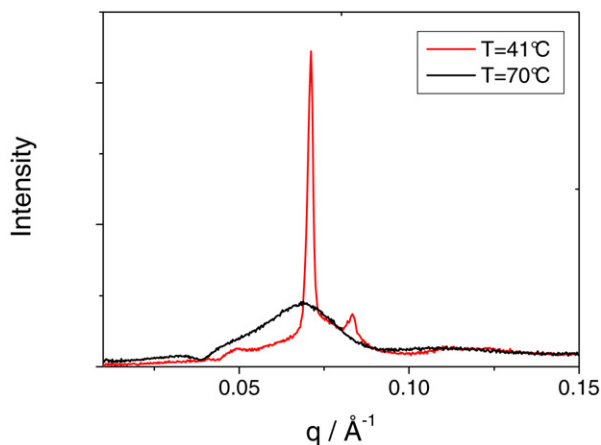


Fig. 4. SAXS profiles of 30 wt% 50/50 P85/P123 solution at the temperatures indicated.

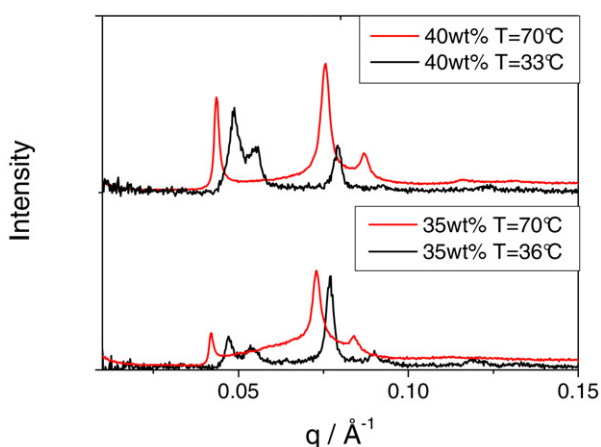


Fig. 5. SAXS profiles of 35 wt% and 40 wt% 50/50 P85/P123 50/50 at the temperatures indicated.

copolymer, although it decreases for the 50 wt% system. The gel phase region is bounded at high temperature for the 30–45 wt% gels inclusive, although not clearly for the 50 wt% system. For the 30–45 wt% solutions the non-zero modulus at high temperature, above the transition from the lower temperature gel, is consistent with the formation of a softer gel structure.

### 3.2. Phase behaviour—SAXS

Small-angle scattering was used to determine the structure of the gels and solutions. Peak assignments from a number of SAXS and experiments are listed in Table 2. Figs. 4–8 highlight some of the data. The 50/50 P85/P123 solutions are considered first, followed by the parent homopolymers (P85 has been studied extensively by SANS [18], the mapping of the phase behaviour of P123 [21] is incomplete). Fig. 4 shows SAXS data for 30 wt% solutions. Neglecting a small feature around  $q = 0.05 \text{ \AA}^{-1}$ , the peaks observed at  $q^*$  and  $\sqrt{4/3}q^*$  are consistent with an FCC/HCP structure at  $T = 41^\circ\text{C}$ . However, the  $q^*$  value is significantly different from that at other concentrations. If the small peak at  $0.05 \text{ \AA}^{-1}$  is included in the indexation, it would indicate a cubic structure other than FCC/HCP, in fact probable BCC symmetry. This seems very unlikely given the relative peak intensities. It appears most likely that the initial cubic gel structure may have a lattice constant differing from that for 35 wt% and higher concentration copolymer gels, for which  $q^* = 0.048 \pm 0.01 \text{ \AA}^{-1}$ . At high temperature, there is a single maximum in the scattered intensity, indicating a structure

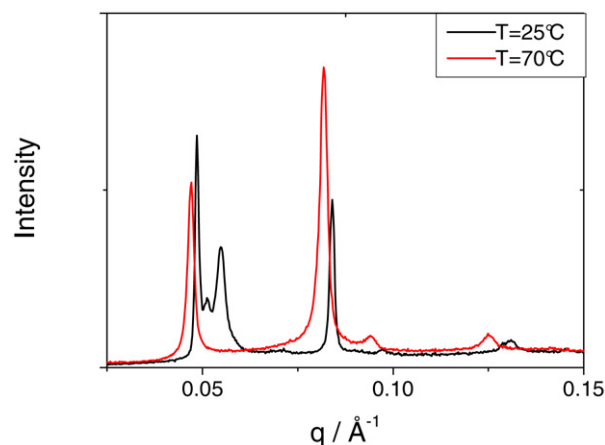


Fig. 6. SAXS profiles of a 45 wt% 50/50 P85/P123 solution.

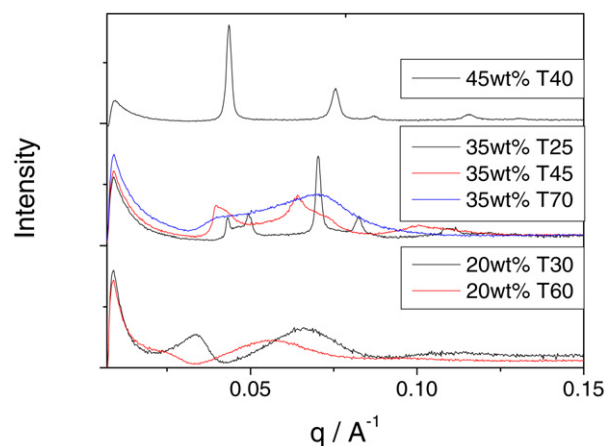


Fig. 7. SAXS profiles of 20 wt%, 35 wt% and 40 wt% solutions of P123.

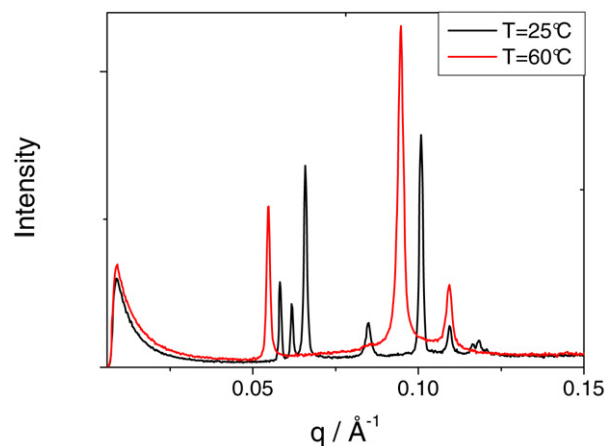


Fig. 8. SAXS profiles of a 40 wt% solution of P85 at the temperatures indicated.

without well-defined lattice order but with a structure factor maximum. This is assigned to a cylindrical micelle structure, not fully ordered into a hexagonal lattice. At 35 wt% copolymer and above, the hexagonal structure of cylindrical micelles at high temperature is well defined (Fig. 5). At low temperature, a cubic structure is observed in the clear, hard gel region (Fig. 2)—this can be indexed to a normal FCC structure for the 40 wt% gel, for which the intensity of the observed orders of reflection decreases monotonically with  $q$ . However for the 35 wt% gel, although the peaks can be indexed to an FCC structure, the intensity of the peaks is anomalous, in that

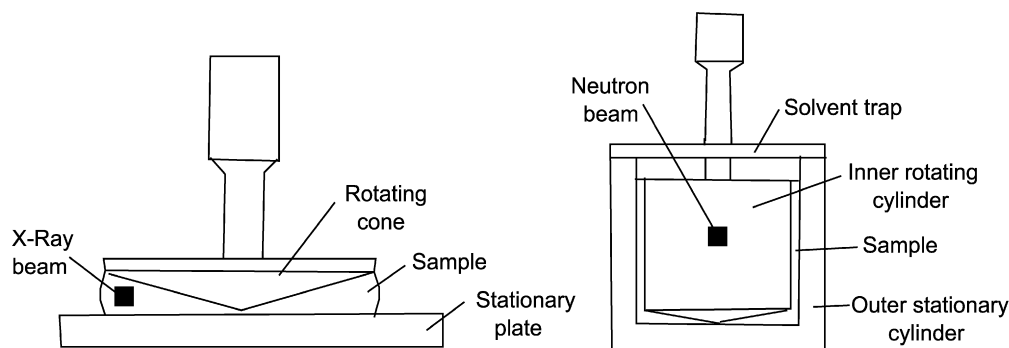


Fig. 9. Geometries used in rheo-SAXS experiments: (left) cone-and-plate; (right) Couette.

the third order is more intense than the first. Since the third order peak is close to that for the high temperature hexagonal structure, we suspect this indicates either that the system contains a fraction of the higher temperature structure (due to the heat/cool protocol employed) or there is preferential alignment of the gel along a particular flow axis. For the 40 wt% gel, the peak position of the first order 111 reflection indicates a unit cell size of 22.2 nm. Assuming an FCC/HCP packing fraction  $\pi/(3\sqrt{2}) = 0.74$ , this leads to an estimated micellar radius  $R = 7.8$  nm. This is in good agreement with the hydrodynamic radius from DLS in dilute solution, especially considering that  $R_h/R$  is expected to be greater than unity for particles that do not behave as perfect hard spheres [22].

Representative SAXS profiles for 45 wt% gels are shown in Fig. 6. At 25 °C, the peaks are consistent with an FCC structure (there is a small additional peak between the  $q^*$  and  $\sqrt{4/3}q^*$  peaks) and at high temperature, the data indicate a hexagonal structure.

Since there have been few small-angle scattering studies on P123, we also present some results on this. Fig. 7 contains selected data. The data for the 20 wt% solution suggest a micellar solution, the presence of a structure factor peak especially at low temperature indicates significant inter-micellar interactions. Similar data have been reported previously as part of a study of P123 in ternary mixtures with ethanol and water [21]. The data for the 35 wt% solution point to the formation of an FCC cubic structure at 25 °C which persists up to around 40 °C, there being an ill-defined structure at 45 °C close to the phase boundary followed by a diffuse structure of cylindrical micelles not ordered on a hexagonal lattice at high temperature. The 40 wt% solution is hexagonal at 40 °C, supporting the downward curvature with increasing concentration of the phase boundary in Fig. 1b, in contrast to that for the mixture in Fig. 2.

Fig. 8 presents SAXS data for the 40 wt% gel of P85. According to Fig. 1a, a cubic phase may be expected at low temperature followed by a hexagonal phase at higher temperature. Indeed the results point to a predominantly cubic structure at 25 °C and a hexagonal phase at 70 °C. In fact 25 °C is very close to a phase boundary, and the SAXS pattern seems to correspond to a coexistence of FCC cubic and hexagonal structures. In regard to the observed FCC structures for this and related Pluronics, it may be noted that Mortensen et al. have recently reported that commercial samples of Pluronic F127 form FCC gels, however removal of PEO–PPO diblock impurities leads to the formation of BCC phases [23]. It is possible that this will impact on the cubic phase behaviour for P85 and P123.

The main difference in the phase diagram for the mixed P85/P123 system is the presence of the cubic phase at low temperatures and concentrations above 40 wt%, in contrast to the phase behaviour of the parent polymers. The formation of cylindrical micelles by block copolymers is usually associated with the release of molecular packing constraints in spherical micelles when the

chains would become too stretched [7]. This may be relieved in the mixed micellar system since the shorter P85 chains (with much shorter hydrophobic PPO block) can relieve the packing of the P123 chains. The increase in micelle hydrodynamic radius observed for the mixed system is consistent with this viewpoint.

### 3.3. Shear alignment

SAXS and SANS were used to probe the orientation of hexagonal and cubic phases of the P85/P123 mixtures under steady shear, using both Couette and cone-and-plate geometries, as illustrated in Fig. 9. The Couette geometry was used for soft gels in the hexagonal phase, the cone-and-plate geometry was required for hard gels which have a rather high elastic modulus (Fig. 2).

Fig. 10a shows SANS data for the 40 wt% mixture, subjected to steady shear at  $= 0.1 \text{ s}^{-1}$  at 70 °C (left). Preferential vertical orientation in the observed ring of scattering can be observed. This is consistent with shear-induced alignment of hexagonal-packed cylinders along the horizontal flow direction. Much enhanced alignment is observed for the 45 wt% mixture (Fig. 10b). A first order peak at  $q^* = 0.0457 \text{ \AA}^{-1}$  is accompanied by higher order reflections at  $0.0789 \text{ \AA}^{-1}$  and  $0.0904 \text{ \AA}^{-1}$ , i.e. at  $\sqrt{3}q^*$  and  $\sqrt{4}q^*$ , consistent with an aligned hexagonal phase.

For the cubic hard gels, shearing in the Couette cell was not possible. Both “hand shearing” and shearing in a cone-and-plate cell were successfully used to orient the gels. Fig. 11 shows SANS data for a HCP/FCC gel in a 40 wt% mixture, obtained by “hand shearing.” A high degree of alignment was achieved by this method. Six well defined reflections are evident, these are distorted somewhat from the expected hexagonal symmetry due to distortions in the hexagonal lattice introduced by the shearing protocol. Better control over the shearing conditions can be achieved using the cone-and-plate cell and *in situ* SAXS/rheology experiments were carried out to examine the shear-induced orientation of the cubic phase of a 30 wt% mixture. These experiments were performed with the beam collimated to around 50  $\mu\text{m}$  square. The sample was mounted in a cone-and-plate cell ( $1^\circ$  cone, 50 mm radius). The X-ray beam was passed through the cone in the tangential configuration as shown in Fig. 9 (the rheometer was actually tilted in the experiment so that the inner cone edge was horizontal). The calculated gap at this edge of the cone-and-plate is 436  $\mu\text{m}$ . On scanning the sample across the gap and also horizontally along the shear gradient direction we observed changes in orientation of the specimen even in the absence of shear. These result from alignment of the cubic gel structure caused by compression on loading the sample into the cell. Fig. 12 shows a SAXS pattern for an aligned 30 wt% sample obtained in this way. A very well defined “monocrystal” exhibiting a HCP structure can be deduced [24]. The pattern is misaligned with respect to the vertical by  $54^\circ$ . We believe this results from flow alignment along the [111] direction (FCC notation), with a SAXS pattern defined with respect

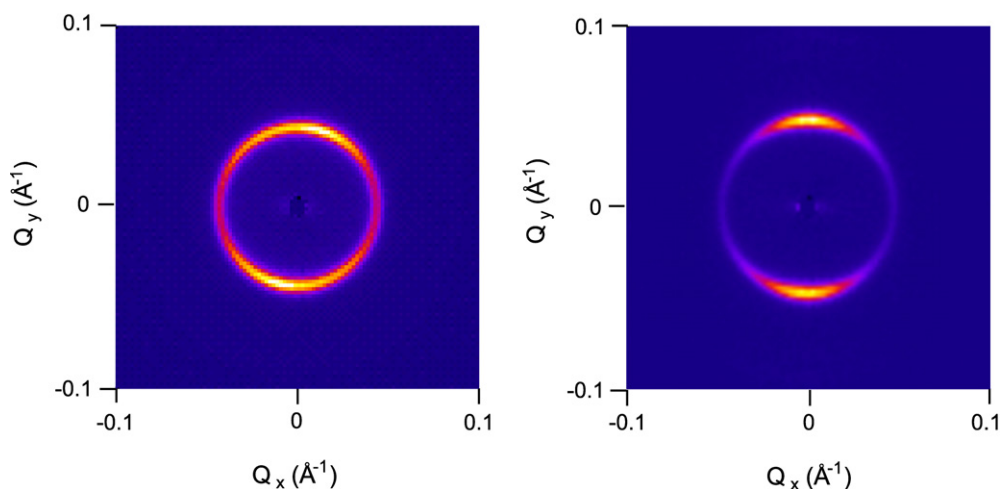


Fig. 10. SANS patterns of (left) 40 wt% 50/50 P85/P123, sheared at  $0.1 \text{ s}^{-1}$  at  $70^\circ\text{C}$ , (right) 45 wt% P85/P123 50/50, sheared at  $10 \text{ s}^{-1}$  at  $75^\circ\text{C}$ .

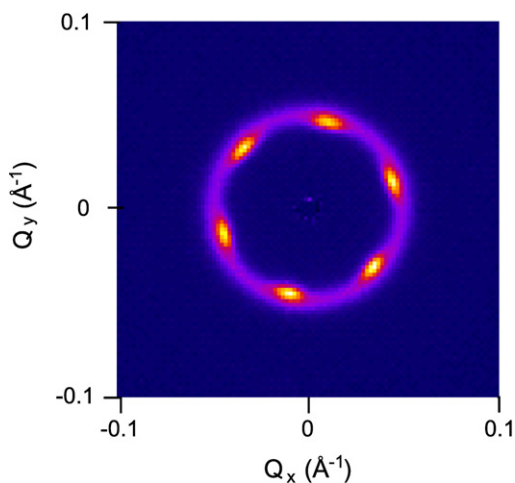


Fig. 11. SANS pattern of 40 wt% 50/50 P85/P123, hand sheared at  $25^\circ\text{C}$ .

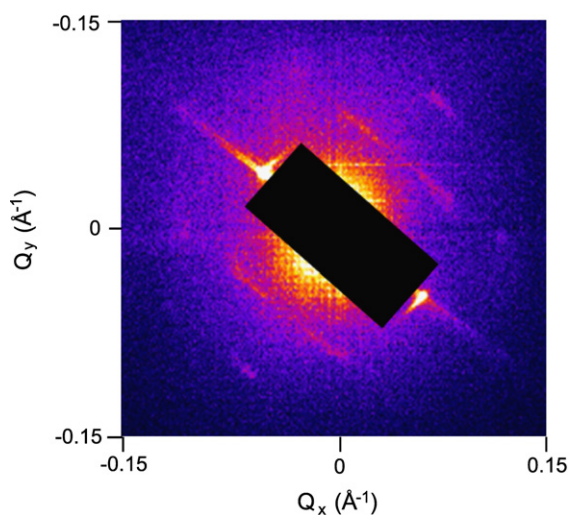


Fig. 12. SAXS pattern from 30 wt% 50/50 P85/P123 sheared at  $20^\circ\text{C}$ .

to a [002] direction. After control experiments using an unfilled cell and more dilute solutions of our copolymer mixture (which do not form cubic gels) we suspect that the flares evident in Fig. 12 result from microscopic bubbles trapped in the gel and aligned along the [002] direction.

#### 4. Summary

Mixed micelles are formed in 50/50 mixtures of P85/P123 with a larger size than that of the parent polymers due to the higher packing density of the block copolymer chains that can be achieved, leading to an increased association number. This in turn affects the gel phase diagram—cubic phases of packed spherical micelles exist at high concentration for the mixed system but not for P85 or P123 on their own, in which case hexagonal phases of cylindrical phases are formed. The formation of cylindrical micelles results from the relief of chain stretching constraints in spherical micelles due to the formation of micelles with cores comprising two populations of PPO chain lengths, differing by nearly a factor of two in chain length. The structure of the cubic phase in the mixed system is FCC/HCP. The phase boundaries were mapped via small-angle X-ray and neutron scattering, complemented by shear rheometry and mobility (tube inversion) tests with visual inspection of clouding. Finally, shear alignment was investigated using a novel rheo-SAS system comprising either Couette or cone-and-plate geometries. The hexagonal phase can be aligned by application of steady shear in the Couette geometry. Reciprocating hand shearing could be used to align the hard gel, which was also oriented upon compression in a cone-and-plate cell (however subsequent shearing led to a decrease in orientation). Our system exhibits quite distinct behaviour to mixtures of Pluronic copolymers with similar P block lengths but different E chain lengths. In the case of P123/F127, addition of P123 chains with shorter E blocks reduces the stability of the cubic gel phase. Our study also differs from recent work on mixtures of telechelic polymers, which have a reversed architecture with outer hydrophobic blocks [25]. Our results point to strategies to modify the structural, and hence rheological, properties of Pluronic block copolymers, in particular by enhancing the concentration region over which the cubic gel phase is stable. This may be useful in biomedical and personal care product applications.

#### Acknowledgments

The authors would like to thank the STFC for the award of SANS beam time at ISIS (experiment number RB72006) and SAXS beam time at the SRS (beamtime Ref. 49003) and Diamond Light Source. They would also like to acknowledge the technical assistance provided by Mr Lawrence Harper of Anton-Parr Ltd.

## References

- [1] B. Jönsson, B. Lindman, K. Holmberg, B. Kronberg, *Surfactants and Polymer in Aqueous Solution*, Wiley, Chichester, 1998.
- [2] M.W. Edens, R.H. Whitmarsh, in: I.W. Hamley (Ed.), *Developments in Block Copolymer Science and Technology*, Wiley, Chichester, 2004, p. 325.
- [3] P. Alexandridis, J.F. Holzwarth, T.A. Hatton, *Macromolecules* 27 (1994) 2414.
- [4] M.W. Edens, in: V.N. Nace (Ed.), *Nonionic Surfactants: Polyoxyalkylene Block Copolymers*, vol. 60, Marcel Dekker, New York, 1996, p. 185.
- [5] B. Chu, Z. Zhou, in: V.M. Nace (Ed.), *Nonionic Surfactants: Polyoxyalkylene Block Copolymers*, vol. 60, Marcel Dekker, New York, 1996.
- [6] P. Alexandridis, *Curr. Opin. Colloid Interface Sci.* 2 (1997) 478.
- [7] I.W. Hamley, *Block Copolymers in Solution*, Wiley, Chichester, 2005.
- [8] N. Jain, K. Contractor, P. Bahadur, *J. Surf. Sci. Technol. B* 13 (1997) 89.
- [9] S. Gaisford, A.E. Beezer, J.C. Mitchell, *Langmuir* 13 (1997) 2606.
- [10] C. Chaibundit, N.M.P.S. Ricardo, F.D.L.L. Costa, S.G. Yeates, C. Booth, *Langmuir* 23 (2007) 9229.
- [11] T. Liu, V.M. Nace, B. Chu, *Langmuir* 15 (1999) 3109.
- [12] T. Liu, B. Chu, *J. Appl. Crystallogr.* 33 (2000) 727.
- [13] W. Mingvanish, C. Chaibundit, C. Booth, *Phys. Chem. Chem. Phys.* 4 (2002) 778.
- [14] N.M.P.S. Ricardo, C. Chaibundit, Z. Yang, D. Attwood, C. Booth, *Langmuir* 22 (2005) 1301.
- [15] S.W. Provencher, *Comput. Phys. Commun.* 27 (1982) 229.
- [16] C.C. Tang, C.M. Martin, D. Laundry, S.P. Thompson, G.P. Diakun, R.J. Cernik, *Nucl. Instrum. Methods Phys. Res. Sect. B* 222 (2004) 659.
- [17] R.J. Cernik, P. Barnes, G. Bushnell-Wye, A.J. Dent, G.P. Diakun, J.V. Flaherty, G.N. Greaves, E.L. Heeley, W. Helsby, S.D.M. Jacques, J. Kay, T. Rayment, A.J. Ryan, C.C. Tang, N.J. Terrill, *J. Synch. Rad.* 11 (2004) 163.
- [18] K. Mortensen, *J. Phys. Condens. Matter* 8 (1996) A103.
- [19] K. Mortensen, J.S. Pedersen, *Macromolecules* 26 (1993) 805.
- [20] W.J. Harrison, G.J. Aboulgasem, F.A.I. Elathrem, S.K. Nixon, D. Attwood, C. Price, C. Booth, *Langmuir* 21 (2005) 6170.
- [21] S.S. Soni, G. Brotons, M. Bellour, T. Narayanan, A. Gibaud, *J. Phys. Chem. B* 110 (2006) 15157.
- [22] I.W. Hamley, C. Daniel, W. Mingvanish, S.-M. Mai, C. Booth, L. Messe, A.J. Ryan, *Langmuir* 16 (2000) 2508.
- [23] K. Mortensen, W. Batsberg, S. Hvidt, *Macromolecules* 41 (2008) 1720.
- [24] F.R. Molino, J.-F. Berret, G. Porte, O. Diat, P. Lindner, *Eur. Phys. J. B* 3 (1998) 59.
- [25] F. Renou, L. Benyahia, T. Nicolai, O. Glatter, *Macromolecules* 41 (2008) 6523.
- [26] W. Brown, K. Schillén, M. Almgren, S. Hvidt, P. Bahadur, *J. Phys. Chem.* 95 (1991) 1850.
- [27] G. Wanka, H. Hoffmann, W. Ulbricht, *Macromolecules* 27 (1994) 4145.